



OPEN ACCESS

EDITED BY

Abby Green,
Washington University in St. Louis,
United States

REVIEWED BY

Mani Larijani,
Simon Fraser University, Canada
Simon Baker,
University of York, United Kingdom

*CORRESPONDENCE

Linda Chelico,
✉ linda.chelico@usask.ca

RECEIVED 30 March 2023

ACCEPTED 22 May 2023

PUBLISHED 01 June 2023

CITATION

Granadillo Rodríguez M, Wong L and Chelico L (2023), Similar deamination activities but different phenotypic outcomes induced by APOBEC3 enzymes in breast epithelial cells.
Front. Genome Ed. 5:1196697.
doi: 10.3389/fgeed.2023.1196697

COPYRIGHT

© 2023 Granadillo Rodríguez, Wong and Chelico. This is an open-access article distributed under the terms of the [Creative Commons Attribution License \(CC BY\)](https://creativecommons.org/licenses/by/4.0/). The use, distribution or reproduction in other forums is permitted, provided the original author(s) and the copyright owner(s) are credited and that the original publication in this journal is cited, in accordance with accepted academic practice. No use, distribution or reproduction is permitted which does not comply with these terms.

Similar deamination activities but different phenotypic outcomes induced by APOBEC3 enzymes in breast epithelial cells

Milaid Granadillo Rodríguez, Lai Wong and Linda Chelico*

Department of Microbiology and Immunology, University of Saskatchewan, Saskatoon, SK, Canada

APOBEC3 (A3) enzymes deaminate cytosine to uracil in viral single-stranded DNA as a mutagenic barrier for some viruses. A3-induced deaminations can also occur in human genomes resulting in an endogenous source of somatic mutations in multiple cancers. However, the roles of each A3 are unclear since few studies have assessed these enzymes in parallel. Thus, we developed stable cell lines expressing A3A, A3B, or A3H Hap I using non-tumorigenic MCF10A and tumorigenic MCF7 breast epithelial cells to assess their mutagenic potential and cancer phenotypes in breast cells. The activity of these enzymes was characterized by γ H2AX foci formation and *in vitro* deamination. Cell migration and soft agar colony formation assays assessed cellular transformation potential. We found that all three A3 enzymes had similar γ H2AX foci formation, despite different deamination activities *in vitro*. Notably, in nuclear lysates, the *in vitro* deaminase activity of A3A, A3B, and A3H did not require digestion of cellular RNA, in contrast to that of A3B and A3H in whole-cell lysates. Their similar activities in cells, nonetheless, resulted in distinct phenotypes where A3A decreased colony formation in soft agar, A3B decreased colony formation in soft agar after hydroxyurea treatment, and A3H Hap I promoted cell migration. Overall, we show that *in vitro* deamination data do not always reflect cell DNA damage, all three A3s induce DNA damage, and the impact of each is different.

KEYWORDS

APOBEC3, cancer, deaminase, DNA damage, enzyme activity

1 Introduction

The human APOBEC3 (A3) enzymes belong to the APOBEC family and consist of seven members (A3A, A3B, A3C, A3D, A3F, A3G, and A3H) that deaminate cytosine to form uracil on single-stranded (ss) DNA (Refsland and Harris, 2013). Since uracil templates for the addition of adenosine or initiates base excision repair (BER) to remove the uracil, these enzymes are promutagenic. Normally, this is used as an intrinsic barrier to retroviruses, endogenous retroelements, and some DNA viruses where A3-induced uracils in these genomes cause their inactivation or degradation (Arias et al., 2012; Feng et al., 2014; Cheng et al., 2021). Accordingly, A3 enzymes are normally only highly expressed in germ cells, lymphoid cells, and epithelial cells in response to viral infection (Jarmuz et al., 2002; Koning et al., 2009; Okeoma et al., 2010; Refsland et al., 2010; Milewska et al., 2018; Wei et al., 2020). However, some AID/APOBEC enzymes have also been harnessed as tools in genome editing (Evanoff and Komor, 2019). Acting as cytosine base editors (CBEs) by linking an AID/APOBEC enzyme to catalytically inactive CRISPR-Cas9, the formation of uracil by AID/

APOBEC catalysis can be used to induce C→T mutations in somatic cells (Komor et al., 2016; St Martin et al., 2018; McGrath et al., 2019; Liu et al., 2020; Zhao et al., 2021). However, their off-target effects need to be controlled. This is especially important since A3 enzymes are a source of somatic mutations in at least 70% of cancer types, with 25%–50% of sequenced tumor genomes containing A3-induced mutations (Petljak and Alexandrov, 2016; Alexandrov et al., 2020; Bergstrom et al., 2022). Understanding the natural mutagenic potential of A3 enzymes in the genome can inform research on their roles as CBEs and improve our understanding of the origins of somatic mutations in tumor cells.

To induce mutations in genomic DNA, it is important that the enzymes localize to the nucleus, but the enzymes must also be able to compete for ssDNA with Replication Protein A (RPA) during dynamic and transient processes such as replication, transcription, and DNA repair (Swanton et al., 2015; Adolph et al., 2017b; Mertz et al., 2017; Adolph et al., 2018; Green and Weitzman, 2019; Wong et al., 2021). Only A3A, A3B, A3C, and A3H can enter the nucleus (Vieira and Soares, 2013). A3G can enter the nucleus in certain cancer cells after ionizing radiation treatment (Nowarski et al., 2012; Talluri et al., 2021; Britan-Rosich et al., 2022; Liu et al., 2023). A3H has seven major haplotypes, and although all can enter the nucleus to varying degrees, A3H haplotype I (Hap I) is the only one that is predominantly nuclear (Li and Emerman, 2011; Wang et al., 2011). A3B has a nuclear localization signal (NLS), and A3A and A3C enter the nucleus by diffusion (Bogerd et al., 2006; Chen et al., 2006; Lackey et al., 2012).

To date, only A3A, A3B, and A3H Hap I have been implicated in processes related to somatic mutagenesis and cancer using retrospective data from The Cancer Genome Atlas (TCGA) or other methods where whole-genome sequencing and mRNA expression can be analyzed (Burns et al., 2013a; Middlebrooks et al., 2016; Starrett et al., 2016; Yan et al., 2016; Glaser et al., 2018; Chen et al., 2019; Roper et al., 2019; Hix et al., 2020; Law et al., 2020; Chervova et al., 2021; Petljak et al., 2022). Suppression of A3 mRNA transcription provides the main protective measure against somatic mutagenesis, although A3B and A3A transcription is upregulated in response to DNA replication stress, an early sign of cellular transformation and viral infection (Kanu et al., 2016; Oh et al., 2021). A3A activity also appears to be regulated by binding partners that suppress catalytic activity, such as Human Tribbles 3 or chaperonin-containing TCP-1 (CCT) complex (Aynaud et al., 2012; Green et al., 2021). A3H Hap I is ubiquitinated in cells, and the resulting short half-life decreases its catalytic activity (Chesarino and Emerman, 2020). A3B and A3H Hap I cytidine deaminase activity can also be suppressed by binding cellular RNA, but the implications of this for their activity in the nucleus are not known (Cortez et al., 2019).

The formation of promutagenic uracils through the intrinsic deaminase activity of these enzymes occurs in a sequence-specific manner, and those involved in cancer preferentially deaminate the central cytosine in 5'TCW trinucleotide motifs (where W = A or T on ssDNA) to form uracil (Refsland and Harris, 2013). Uracil-DNA glycosylase (UNG) is a highly conserved repair enzyme that initiates BER and catalyzes the excision of uracil from ssDNA and double-stranded (ds) DNA and prevents mutagenesis from A3 enzymes (Friedberg et al., 2005). In this context, the uracil-DNA glycosylase inhibitor (UGI) protein from bacteriophage PBS2 has been a useful

tool to determine if A3-catalyzed uracils induce DNA damage and mutagenesis (Richardson et al., 2014). Some uracils escape BER and result in C→T mutations when uracil is used as a template during replication or an error-prone process mediated by Rev1 can result in C→G mutations due to insertion of C opposite the abasic site created during BER (Nik-Zainal et al., 2012; Roberts et al., 2012; Chan et al., 2013; Henderson and Fenton, 2015). These two types of mutations form the basis of APOBEC-induced single base substitution (SBS) signatures SBS2 (C→T) and SBS13 (C→G) in cancer genomes (Alexandrov et al., 2013).

A3B was first identified as a significant mutational source in breast cancer (BC) but was later identified in other cancer types, including bladder, cervical, lung, and head-and-neck cancers, where it was evident that there was a positive correlation between A3B expression and the total APOBEC-mutation load (Burns et al., 2013a; Burns et al., 2013b). A3B is overexpressed in almost 50% of BC, the majority of BC cell lines, and was linked to DNA deaminase activity in BC cell extracts (Burns et al., 2013a; Petljak et al., 2022). High A3B expression levels have been associated with poor clinical outcomes for estrogen receptor-positive BC and can promote tamoxifen resistance (Sieuwerds et al., 2014; Law et al., 2016). However, the frequency of A3B mutations is not always correlated with A3B expression levels (Nik-Zainal et al., 2014; Roberts and Gordenin, 2014; Cescon et al., 2015; Petljak et al., 2022). In addition, 22% of humans have a deletion polymorphism resulting in loss of the A3B gene, and sequencing of BC tumors from individuals carrying this deletion indicated that these tumors contained APOBEC-induced mutations at higher abundance than the non-carriers, consistent with recent data in cell lines with artificial A3A or A3B deletions introduced (Kidd et al., 2007; Nik-Zainal et al., 2014; Petljak et al., 2022). Although A3A mRNA levels in BC are much lower than A3B, they are more significantly correlated with BC, and A3A appears to be more active than A3B *in vitro*, suggesting that less steady-state A3A is needed in cells to induce somatic mutagenesis (Cortez et al., 2019; Petljak et al., 2022). This is likely due to the more open conformation of the A3A active site compared to other family members such as A3B or activation-induced cytidine deaminase (AID) (King and Larjani, 2017; Shi et al., 2017). Another study found the A3A mutational footprints in tumors but no corresponding A3A expression and suggested that A3A is upregulated early but later inactivated, perhaps due to being the most active deaminase that could cause cell death through its activity over time, resulting in episodic expression (Landry et al., 2011; Mussil et al., 2013; Chan et al., 2015). In addition, one study of APOBEC-induced mutations from A3B-deleted BC tumors revealed that the only tumors displaying the APOBEC mutation signature also contained at least one allele of A3H Hap I, providing correlative evidence that this enzyme may be the additional source of mutagenesis (Starrett et al., 2016).

The previous studies are not conclusive about the relative contribution of A3A, A3B, and A3H Hap I to BC mutagenesis. A major issue has been the use of retrospective patient samples (Petljak et al., 2019), reliance on mRNA as an indicator of enzyme activity (Jalili et al., 2020), or a lack of studies where A3 enzymes were tested in parallel. This has led to questions of whether APOBEC-induced mutations are drivers or passengers in the overall tumorigenesis process. Most of the previous A3A research was conducted in yeast, cell lines, and *in silico*, but recently there has been direct evidence of

A3A tumorigenic potential *in vivo* (Chan et al., 2015; Glaser et al., 2018; Cortez et al., 2019; Jalili et al., 2020; Law et al., 2020). The mutation signature of A3A is also higher than that of A3B in MDA-MB-453 and BT474 breast carcinoma cell lines (Petljak et al., 2022). Direct comparison of deamination activity of A3A and A3B in whole-cell (WC) lysates of the breast carcinoma cell lines BT474, CAMA-1, and MDA-MB-453 showed that A3A was more active than A3B, but part of the reason for higher activity of A3A is that it was not inhibited by RNA, unlike A3B and A3H Hap I (Cortez et al., 2019).

Although the activities of the A3 enzymes have been characterized in various ways, there is still no comparison of deamination activity in nuclear (Nuc) lysates, where there may be less inhibitory RNA than in WC lysates. In addition, there have been no studies determining if A3-induced mutations cause any specific cancer cell phenotype. Here, we aimed to compare in parallel A3A, A3B, and A3H Hap I. We chose BC as a model because all three of the A3s have been implicated (Burns et al., 2013a; Burns et al., 2013b; Chan et al., 2015; Starrett et al., 2016; Cortez et al., 2019). Using two human breast epithelial cell lines, MCF10A (non-tumorigenic, immortalized mammary epithelial cell line) and MCF7 (tumorigenic), that have borderline undetectable endogenous A3 expression (Burns et al., 2013a), we developed stably transduced cell lines expressing either Flag-tagged A3A, A3B, or A3H Hap I and tested the induced DNA damage, deamination activity, and ability to induce cancer cell phenotypes.

2 Materials and methods

2.1 Cell culture and generation of stable cell lines expressing A3s

The 293T, HCC1428, MCF10A, and MCF7 cell lines were obtained from ATCC and cultured as recommended by ATCC, excluding antibiotics. Lentiviruses were generated by transfection of a pLVX-3x Flag vector with psPAX2 and pMD2.G into 293T cells. The transduction of MCF10A and MCF7 with the resulting lentiviruses expressing Flag-tagged-A3A, -A3B, and -A3H Hap I was performed for 16 h in a medium containing 8 µg/mL polybrene. Transduced MCF10A and MCF7 cells were selected with 1 µg/mL and 2 µg/mL puromycin, respectively, for 7 days and maintained as polyclonal cell lines with 0.25 µg/mL puromycin. Experiments with dox-induced cells were controlled with either transduced cells that were not dox induced or dox-induced non-transduced parental cells.

2.2 Immunoblotting

The MCF10A- and MCF7-derived stable cell lines were incubated for 72 h with doxycycline (dox) concentrations ranging from 0.05 to 2 µg/mL to induce the expression of A3-Flag enzymes. Cells were lysed with 2X Laemmli buffer, and WC and cytoplasmic (Cyt) and Nuc lysates obtained after fractionation were resolved by SDS-PAGE. Antibodies used are labeled on each immunoblot. Secondary detection was performed using LI-COR IRDye antibodies produced in donkey (IRDye 680-labeled anti-rabbit and IRDye 800-labeled anti-mouse). Quantification of band intensities was performed using Odyssey software with normalization of each experimental lane to its respective α -

tubulin, which was detected in parallel on the same blot. The antibodies purchased from Sigma-Aldrich were anti- α -Tubulin antibody, mouse monoclonal (T8203/clone AA13, purified from hybridoma cell culture, Public ID AB_1841230, used at 1:1000); anti- α -Tubulin antibody, rabbit monoclonal (SAB5600206/clone RM113, used at 1:5000); ANTI-FLAG[®] antibody produced in rabbit (F7425, Public ID AB_439687, used at 1:1000); monoclonal ANTI-FLAG[®] M2 antibody produced in mouse (F1804/Clone M2, Public ID AB_262044, used at 1:1000); and anti-HA antibody produced in rabbit (H6908, Public ID AB_260070, used at 1:1000). The antibody purchased from Thermo Fisher Scientific was Histone H2B monoclonal antibody (MA5-31566/Clone GT387, Public ID AB_2787193, used at 1:500). The antibodies purchased from LI-COR Biosciences were IRDye 680RD donkey anti-rabbit IgG secondary antibody (926-68073, Public ID AB_2895657, used at 1:10,000) and IRDye[®] 800CW donkey anti-mouse IgG secondary antibody (926-32212, Public ID AB_621847, used at 1:10,000).

2.3 qRT-PCR

The RNA preparation, cDNA synthesis, and qPCR were carried out according to the work of Refsland et al. (2010). MCF10A and MCF7 parental and derived cell lines were either untreated or treated with dox for 72 h to induce the expression of A3-Flag enzymes or as a mock control. The primers used for A3B, A3C, A3G, and TBP were as reported by Refsland et al. (2010). The primers for A3A and A3H are listed in [Supplementary Table S1](#).

2.4 Immunofluorescence microscopy

MCF10A- and MCF7-derived stable and transduced cell lines were grown on glass slides and treated for 24 or 72 h with dox for the expression of the A3-Flag enzymes and fixed with 100% cold methanol for 20 min. Where indicated, the cells were transfected with an expression vector encoding the bacteriophage PBS2 UGI protein 24 h before the dox induction (Feng et al., 2017). In addition, where indicated, the cells were transduced with catalytic mutants of each A3 enzyme, A3A E72Q, A3B E255Q, or A3H Hap I E56Q. Catalytic mutants were generated by site directed mutagenesis of the pLVX-3x Flag A3 vectors (Wang and Malcolm, 1999). Primers are listed in [Supplementary Table S2](#). After dox treatment, the cells were permeabilized and stained as previously described (Hix et al., 2020). Quantification of cells with γ H2AX foci is based on the counting of 14 fields of view and totaling at least 100 cells per condition per experiment. The antibodies purchased from Sigma-Aldrich were anti-phospho-H2AFX (pSer139) antibody produced in rabbit (SAB4300213, Public ID 10620164, used at 1:200) and monoclonal ANTI-FLAG[®] M2 antibody produced in mouse (F1804/Clone M2, Public ID AB_262044, used at 1:200).

2.5 Deamination assays

Deamination assays were performed using a protocol adapted from the work of Serebrenik et al. (2019). Specifically, WC lysates

were prepared by sonicating 1×10^6 cells in 150 μ L HED buffer [25 mM HEPES, 10% glycerol, 1 mM DTT, and EDTA-free protease inhibitor (Roche, Basel, Switzerland)]. Additionally, 0.1, 0.5, or 5 mM EDTA was added to inhibit nuclease activity. Samples were then centrifuged, and the supernatant was used in 20 μ L deamination reactions with 1 μ M (293T cells transfected with A3B or A3H Hap I expression plasmids), 0.1 μ M (for MCF10A cell lines), or 0.05 μ M (293T cells transfected with A3A expression plasmid) fluorescein-labeled 43 nt ssDNA substrate that was reported by Serebrenik et al. (2019) (Supplementary Table S3), 2 μ L uracil-DNA glycosylase (UDG) (New England Biolabs), 2 μ L UDG buffer (New England Biolabs), 16.5 μ L lysate, and where indicated in methods or figure legends, RNase A (DNase free). Other modifications are detailed below. Deamination reactions were processed by adding NaOH to a final concentration of 250 mM, heating for 10 min at 95°C, and then, adding an equal volume of formamide/EDTA. Samples were resolved on 16% denaturing polyacrylamide gels and analyzed as previously described (Adolph et al., 2017a; Serebrenik et al., 2019).

2.5.1 Deamination activity of cell expressed enzymes

The 293T cells were or were not transfected in a T75 flask using GeneJuice (EMD Millipore) with 1 μ g of pcDNA, pcDNA-A3A-3xHA, and pVIVO-A3H Hap I-HA for 40 h or 2 μ g of pcDNA-A3B-3xHA for 48 h to obtain similar protein levels. For either non-transfected or transfected 293T cells, the RNase A (6 μ g/mL, Roche) was added or not directly to the reaction mixture. MCF10A-derived stable cell lines were treated with dox for 72 h. Dox concentrations were used to achieve similar steady-state protein levels (A3A, 2 μ g/mL; A3B, 2 μ g/mL; A3H Hap I, 0.05 μ g/mL). Prior to performing the deaminase assay for the MCF10A stable cell lines, WC lysates were either pre-treated or not with RNase A (100 μ g/mL) for 15 min at 37°C.

2.5.2 Deamination activity of purified enzymes in Nuc lysates

For the Nuc lysates from the non-transfected 293T cells, the purified enzymes A3A, A3B, or A3H Hap VII were added to the reactions together with 40 U of murine RNase inhibitor (NEB, Ipswich, Massachusetts). The activity of cell lysates was evaluated in reactions containing 85 nt linear or 21 nt hairpin substrates (Supplementary Table S3). For A3A and A3H Hap VII, 100 nM of a substrate containing two TTC motifs was used at a substrate:enzyme ratio of 1:1. For A3B, 500 nM of a substrate containing two ATC motifs was used at a substrate:enzyme ratio of 1:0.5. Reactions were carried out for 1 h, and the S.A. was measured as pmol substrate deaminated/ μ g enzyme/min. Deamination reactions were processed, resolved, and analyzed as previously described (Adolph et al., 2017a; Serebrenik et al., 2019).

2.6 Preparation of whole-cell lysates and cell fractionation

Cells were harvested and either lysed by sonication in HED buffer or with 2X Laemmli buffer to get the WC lysates for deamination or immunoblot, respectively, or were fractionated.

For fractionation, cells were washed with 1X PBS and pelleted by centrifugation at 500 g for 10 min. The cells used were transfected MCF10A or MCF7 cells that were or were not treated with dox and 293T cells that were or were not transfected with A3-expression plasmids. These conditions to prepare the MCF10A and 293T cells are detailed in Section 2.5, Deamination assays. For MCF7 cells, dox concentrations were used to achieve similar protein expression levels (A3A, 1 μ g/mL; A3B, 2 μ g/mL; A3H Hap I, 1 μ g/mL).

The cell pellet was resuspended in Cyt extraction buffer (10 mM HEPES pH 7.4, 10 mM KCl, 1.5 mM MgCl₂, 340 mM sucrose, 0.5 mM EDTA, 1 mM DTT, and EDTA-free protease inhibitor (Roche)). After 10 min of incubation on ice, 12.5 μ L of 10% NP-40 per 1×10^6 cells was added and followed by vortex mixing at high speed for 15 s. The samples were centrifuged at 3,300 x g for 10 min, and the supernatant was saved as Cyt lysate. The remaining pellet was washed once with Cyt extraction buffer and lysed with Nuc extraction buffer [50 mM HEPES pH 7.4, 500 mM NaCl, 1.5 mM MgCl₂, 0.1% NP 40, 0.5 mM EDTA, 1 mM DTT, and EDTA-free protease inhibitor (Roche)] for 30 min at 4°C. After centrifugation at 13,000 x g, the resulting supernatant was saved as Nuc lysate.

2.7 Protein purification

The A3A, A3B, and A3H Hap VII were purified from *Sf9* cells infected with a recombinant baculovirus expressing a GST-tagged A3. Purification and GST-tag cleavage have been previously described (Love et al., 2012; Feng et al., 2015; Adolph et al., 2017b).

2.8 Soft agar assay

MCF10A and MCF7 parental cell lines and cell lines transfected to express Flag-tagged A3s were either untreated or treated for 24 h with 0.05–2 μ g/mL dox. To examine the effect of hydroxyurea (HU) on anchorage-independent growth, MCF10A and MCF7 (parental and A3-expressing cells) were either untreated or treated for 6 h with 2 mM or 12 mM HU, respectively, to stall replication (Supplementary Figures S1, S2). Following these treatments, a cell suspension consisting of 30,000 cells in 0.36% top agar (2x media (DMEM or EMEM), FBS, 4x MEM vitamin solution) was overlaid in duplicate in six-well plates that contained 0.61% bottom agar (2x media, FBS, 4x MEM vitamin solution). Plates were maintained for 3 weeks and topped with media containing dox every 2 days to maintain A3 expression and prevent desiccation. After 3 weeks, colonies were stained with crystal violet, visualized under a microscope, and quantified manually. The experiment was repeated three times, and for each biological replicate, 10 fields were blindly counted.

2.9 Cell migration assay

The effect of A3 expression on the cell migration, in the presence or absence of HU, was evaluated using the QCM™ 24-well colorimetric cell migration assay (Millipore, Burlington, Massachusetts). MCF10A- and MCF7-derived stable cell lines were untreated, treated with dox, or treated with dox + HU. The

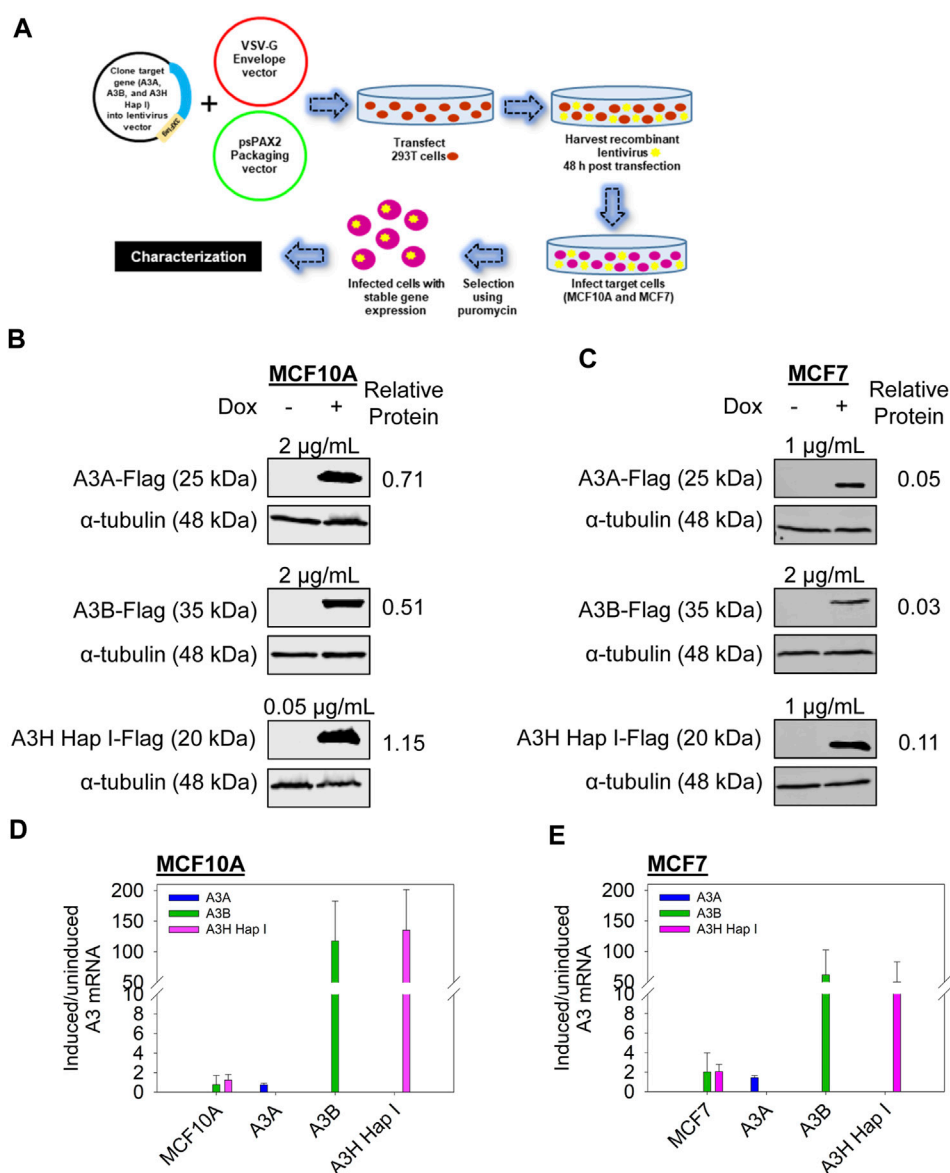


FIGURE 1

A3 protein and mRNA transcript levels in the stable cell lines. (A) Schematic of the generation of the stable cell lines derived from MCF10A and MCF7 cells. (B and C) Steady-state protein levels of A3A, A3B, and A3H Hap I in MCF10A and MCF7 cells. The cells were either uninduced or dox induced for 72 h, and the protein expression was assessed by immunoblot. To obtain similar protein expression levels, the following dox concentrations were used for each cell line: MCF10A A3A (2 µg/mL dox), MCF10A A3B (2 µg/mL dox), MCF10A A3H Hap I (0.05 µg/mL dox), MCF7 A3A (1 µg/mL dox), MCF7 A3B (2 µg/mL dox), and MCF7 A3H Hap I (1 µg/mL dox). Three biologically independent experiments were conducted. Approximate molecular weight (kDa) of each protein is shown based on the closest molecular weight marker band (Supplementary Figure S3). Bands were quantified from one representative experiment, and the Flag intensity was divided by the α -tubulin intensity to account for potential loading differences. Representative results are shown as relative protein levels. Blots were cropped to improve conciseness of the presentation, and uncropped blots are shown in Supplementary Figure S3. (D, E) The mRNA expression measured by qRT-PCR is shown as the fold change of each A3 for induced compared to uninduced conditions after normalization of each to *TBP* expression. Error bars indicate the S.D. from the mean for three biologically independent replicates.

cells were treated with HU twice, on days 3 and 6, and at HU concentrations of 2 mM and 12 mM for MCF10A and MCF7 stable cell lines, respectively. After 7 days of dox treatment, cells were starved for 16 h in media containing 0.5% serum and then seeded (3×10^5 cells) onto the upper chamber in media containing 0.5% serum. Media containing either 0.5% or 10% serum was loaded into the lower chambers. Migration during 48 h toward the lower chamber was determined by colorimetric measurement at 560 nm.

2.10 Statistical analysis

The results are presented as mean \pm standard deviation (S.D.). A two-tailed *t*-test was applied for comparisons of the two groups, while a one-way analysis of variance (ANOVA) followed by the Holm-Sidak *post hoc* test was used for multiple groups. The results were considered statistically significant at a *p*-value of <0.05 . Statistical analyses were performed using SigmaPlot 11.0 software.

3 Results

3.1 A3A, A3B, and A3H Hap I protein expression levels in the stable cell lines

In order to compare the cellular activities of A3A, A3B, and A3H Hap I, we first generated polyclonal MCF10A and MCF7 inducible cell lines to stably express the Flag-tagged A3s (Figure 1A). The cells were then treated with different dox concentrations ranging from 0.05 to 2 $\mu\text{g}/\text{mL}$ to determine the concentration that would induce similar protein expression levels (Figures 1B,C). We were able to obtain similar protein expression for A3A and A3B in MCF10A and MCF7 cells, whereas A3H Hap I expression was slightly higher, even with using lower dox induction levels. This was determined by calculating the relative protein levels after normalizing each Flag band to the α -tubulin in the same lane. The MCF10A- and MCF7-relative protein levels are comparable within each set but not to each other since they were detected on different immunoblots (Supplementary Figure S3).

Using the conditions that had equal A3-Flag expression levels, the mRNA expression levels were assessed by qRT-PCR to determine if there was any expression of endogenous A3 enzymes that could access the nucleus (Figures 1D,E). For the parental, non-transduced MCF10A and MCF7 cell lines, endogenous A3A mRNA was not detected, but there was basal endogenous mRNA expression detected for A3B and A3H Hap I after treatment with dox (Figures 1D,E, MCF10A or MCF7 on *x*-axis). Endogenous low-level A3B expression has previously been detected in these cell lines (Roelofs et al., 2023). After dox induction in transduced cells (labeled A3A, A3B, or A3H Hap I on the *x*-axis), the level of A3A mRNA for both MCF10A and MCF7 cells was low, showing only 0.75- and 1.42-fold increases, respectively, although the steady-state protein expression was similar to A3B (Figures 1B–E). In contrast, A3B mRNA in both transduced cell lines was induced over 60-fold (Figures 1D,E). A3H Hap I mRNA induction in transduced cell lines was over 100-fold in MCF10A cells and 50-fold in MCF7 cells (Figures 1D,E). Even though A3A mRNA expression is lower than A3B and A3H Hap I, low A3A mRNA that provides robust protein levels has been observed in cancer cells; mRNA expression and steady-state protein levels are often not correlated, and importantly, the steady-state protein levels of A3A, A3B, and A3H Hap I are regardless similar in the MCF10A or MCF7 cells (Figures 1B,C) (de Sousa Abreu et al., 2009; Vogel and Marcotte, 2012; Cortez et al., 2019; Jalili et al., 2020; Petljak et al., 2022). Although mRNA expression differences may not be expected with cDNA, this could have occurred if the polyclonal outgrowth was selected against high A3A mRNA-producing cells that had a leaky expression, as they could cause cell death (Green et al., 2016). We also determined if A3C or A3G mRNA were expressed in MCF10A or MCF7 non-transduced cells since they are the only other A3 enzymes with access to the nucleus (Lackey et al., 2013; Liu et al., 2023). However, we did not detect any A3C or A3G mRNA (data not shown).

3.2 A3A, A3B, and A3H Hap I localize to the nucleus and induce γH2AX foci formation

We assessed the A3 localization and ability to induce DNA damage by immunofluorescence microscopy (Figure 2A). We

included the non-transduced parental cells exposed to dox as the mock and also dox-uninduced and -induced conditions for the stable cell lines. For MCF10A- and MCF7- derived stable cell lines, immunofluorescence microscopy showed that A3A and A3H Hap I localized to the nucleus and cytoplasm, but A3B localized only to the nucleus (Figures 2B–G). To determine the γH2AX foci formation, which is a marker of stalled replication forks and dsDNA breaks, we analyzed cells by immunofluorescence microscopy 72 h post dox induction (Figure 2). All cell lines were also either transfected or not with a plasmid expressing UGI to demonstrate that the γH2AX foci were caused by the removal of uracil by UNG. As a further control that the γH2AX foci were caused by A3-catalyzed deaminations, we also transduced cells with a catalytic mutant of A3A (E72Q), A3B (E255Q), or A3H Hap I (E56Q) (Figures 2B–G). The expression of A3A, A3B, and A3H Hap I in either MCF10A or MCF7 cells induced similar pan nuclear γH2AX staining that was blocked for A3-expressing cells that were also expressing UGI demonstrating that γH2AX foci formation was due to formation of A3-catalyzed uracils (Figures 2B–G). There were no γH2AX foci for any of the cells expressing the catalytic mutants of the A3 enzymes (Figures 2B–G).

Previous studies have found different activities between A3A, A3B, and A3H Hap I, but these three enzymes have never been tested in parallel (Burns et al., 2013a; Burns et al., 2013b; Chan et al., 2015; Starrett et al., 2016; Cortez et al., 2019). Thus, to determine if there are any differences in the A3 activity in cells, we detected γH2AX foci after 24 h since the effect of the A3s appeared saturated at 72 h (Figure 2). After 24 h, we detected, on average, γH2AX foci formation in 47% of A3A-, 62% of A3B-, and 64% of A3H Hap I-expressing MCF10A cells (Figure 3A; Supplementary Figure S4). These data demonstrate that the formation of γH2AX foci from cytosine deamination is similar for all three A3 enzymes. For MCF7 cells, we detected γH2AX foci formation in 35% of A3A-, 51% of A3B-, and 17% of A3H Hap I-expressing cells (Figure 3B; Supplementary Figure S4). For A3H Hap I in MCF7 cells, the formation of γH2AX foci was ~ 2 -fold slower, and detection at 72 h showed similar γH2AX foci to A3A and A3B after 24 h (56%, Figures 3B,C; Supplementary Figure S5). Since A3H Hap I is more rapidly ubiquitinated and degraded than other A3H haplotypes, we hypothesize that this process may occur more rapidly in MCF7 cells than in MCF10A cells, resulting in slower accumulation of γH2AX foci (Chesarino and Emerman, 2020). Altogether, the results indicated that A3A, A3B, and A3H Hap I were all able to induce DNA damage in cells at equal amounts in MCF10A cells by 24 h and in MCF7 cells by 72 h.

3.3 RNA in the nucleus does not inhibit A3A, A3B, or A3H cytosine deamination

Cytoplasmic RNA is known to inhibit A3B and A3H Hap I enzyme activity, and this has led to the conclusion that A3A is likely more active in cells due to a lack of RNA inhibition (Cortez et al., 2019). However, the effect of RNA in the nucleus has not been studied. Based on our observation of γH2AX foci formation with all three A3s (Figures 2, 3), we hypothesized that there is less inhibition of A3 activity in the nucleus because there is less RNA. However, before testing our hypothesis, we first wanted to reconcile the

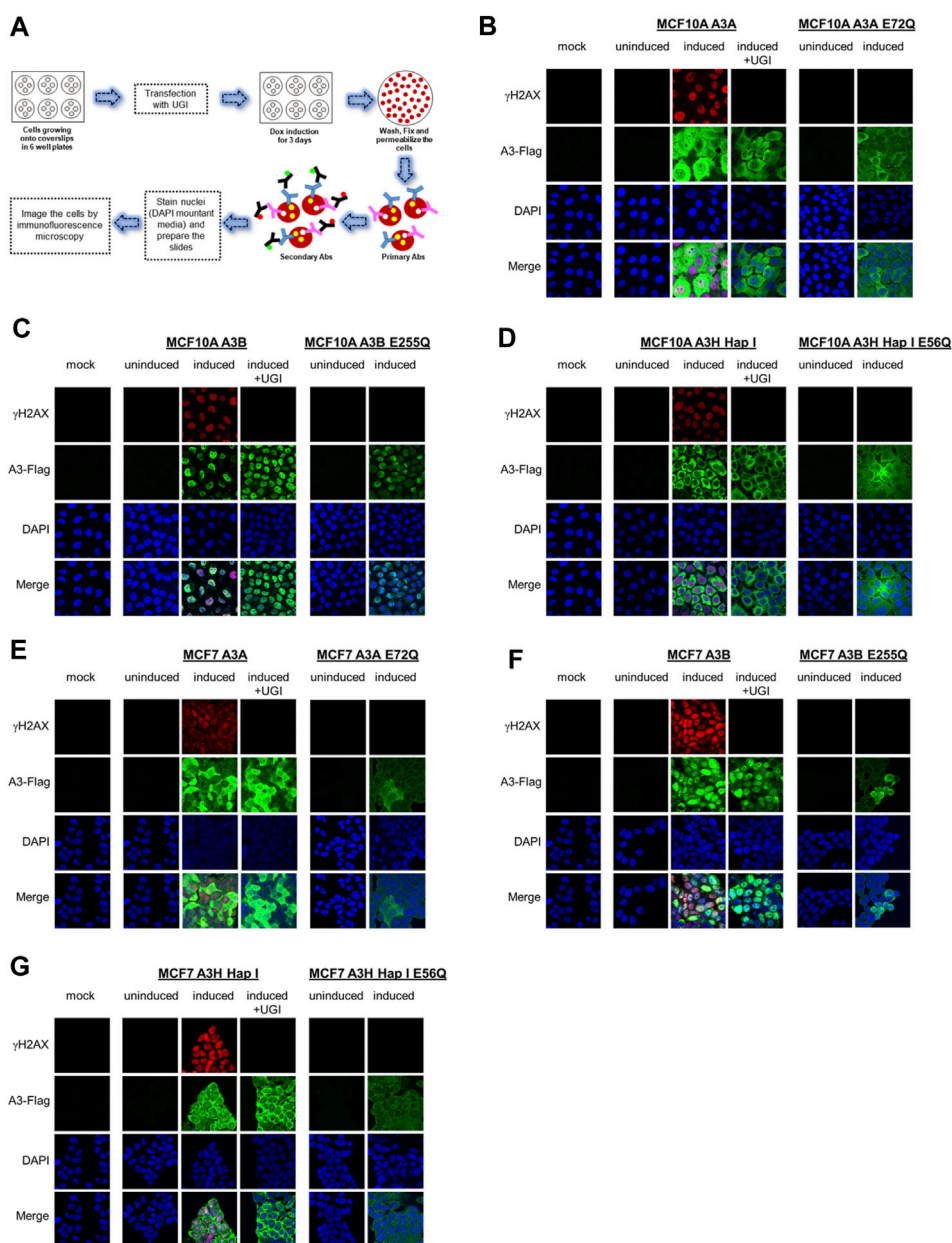


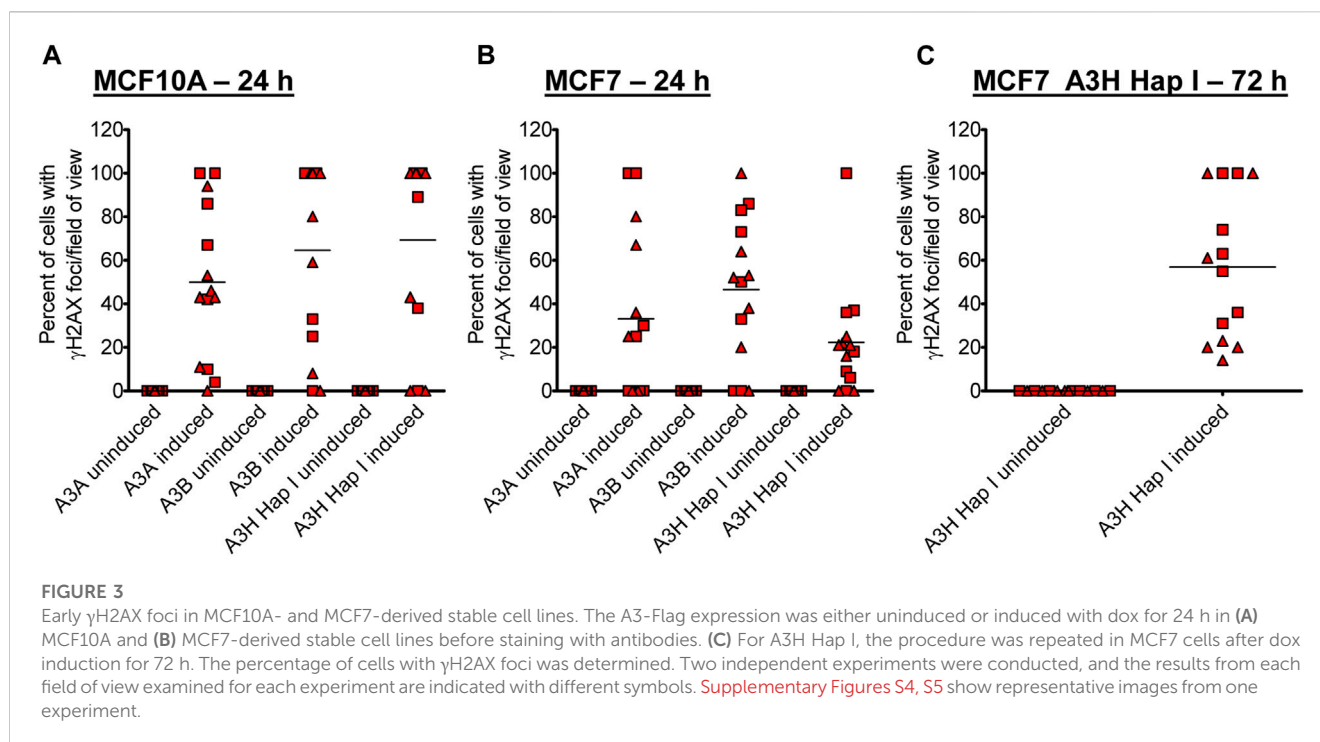
FIGURE 2

γ H2AX foci formation by A3A, A3B, and A3H Hap I. (A) Schematic representation of the protocol followed to assess the protein localization and γ H2AX foci formation by immunofluorescence microscopy using antibodies (Abs). (B–D) The MCF10A cell line was not transfected and treated with dox for 72 h (mock), transfected to express A3A, A3B, or A3H Hap I and not treated with dox for 72 h (uninduced), transfected to express A3A, A3B, or A3H Hap I and treated with dox for 72 h (induced) without or with transfection of a UGI expression plasmid (induced + UGI), transiently transfected with catalytic mutants of A3A (E72Q), A3B (E255Q), or A3H Hap I (E56Q) and not treated with dox for 72 h (uninduced), and transiently transfected with catalytic mutants of A3A (E72Q), A3B (E255Q), or A3H Hap I (E56Q) and treated with dox for 72 h (induced). Green identifies Flag-tagged A3 enzymes, red indicates γ H2AX foci formation, and blue indicates nuclei staining. (E–G) MCF7 parental cell line and MCF7-derived stable cell lines were subjected to same treatments as for the MCF10A cell lines.

γ H2AX foci formation data with previous *in vitro* data showing different A3 activities. We used 293T cells and transfected a known amount of A3-expression plasmid and calculated a specific activity based on the pmol of substrate deaminated per μ g of plasmid transfected per minute (Figure 4A). Consistent with previously published results in other cell line WC lysates, A3A cytidine deaminase activity was not affected by addition of RNase A, but

activity was completely abolished for both A3B and A3H Hap I if the WC lysates were not treated with RNase A. This was also observed in MCF10A cells (Supplementary Figure S6).

To test levels of A3 deamination in Nuc lysates, we used 293T cells. We added purified A3A, A3B, and A3H Hap VII [a stabilized form of A3H Hap I for *in vitro* work (Adolph et al., 2017b)] to untransfected 293T Nuc lysates since noncomparable



amounts of A3A, A3B, and A3H Hap I were found when Nuc lysates were fractionated from 293T cells and especially from MCF10A and MCF7 cells ([Supplementary Figures S7, S8](#)). We then calculated the specific activity based on the pmol of substrate deaminated per μ g of enzyme per minute ([Figure 4B](#)). Longer 85 nt substrates containing the preferred 5'ATC (A3B) or 5'TTC (A3A and A3H) motifs were used to ensure optimal deamination conditions. While A3A prefers hairpin substrates, we did not use a hairpin substrate for comparison between the three enzymes since A3B and A3H do not deaminate hairpin substrates efficiently ([Supplementary Figure S9](#)). Equal volumes of the same Nuc lysates were used for each biological experiment for A3A, A3B, and A3H Hap VII, which ensured that RNA and other nuclear proteins and/or factors were at the same level in each reaction.

The 85 nt substrate had an internal fluorescein label to detect all possible deaminations. Deaminations that occurred at only the 5' site would result in a 67 nt fragment on the gel. Deaminations that occurred at only the 3' site would result in a 48 nt fragment on the gel. Deaminations that occurred at both the 5' and 3' sites on the same ssDNA would result in a 30 nt fragment on the gel. This type of substrate is useful for determining if the enzyme deaminates processively, meaning that more than one deamination on the same ssDNA substrate was catalyzed. A3A was able to deaminate the DNA in Nuc lysates treated or not with RNase A, although the activity in the absence of RNase A was approximately 5-fold less than that with no lysate ([Figure 4B](#), left panel). Similar results were found on the hairpin substrate ([Supplementary Figure S9](#)). In contrast to the WC lysate data, there was no requirement for RNase A for deamination activity in Nuc lysates for A3H Hap VII ([Figure 4B](#), left panel) and A3B ([Figure 4B](#), right panel), although the activity was approximately 2- or 7-fold less than A3A, respectively. The A3H Hap VII and A3B activities were 3-

fold and 2-fold less in the Nuc lysate than in no lysate in the absence of RNase A, respectively ([Figure 4B](#)). Nonetheless, these data corroborate our hypothesis that in the nucleus, compared to WC lysates, there is less inhibition by RNA for A3B and A3H Hap VII. Notably, A3B and A3H Hap VII, which are processive enzymes that usually have the ability to deaminate both cytosines on the same DNA, resulting in a 30 nt band, were unable to do so under the single hit conditions of the experiment ([Figure 4B](#)) ([Feng et al., 2015](#); [Adolph et al., 2017b](#)). Single-hit conditions result when less than 15% of the substrate is used in the reaction and enable conclusions to be made about single ssDNA enzyme encounters ([Creighton et al., 1995](#)). The A3A is not processive, and a 30 nt band was not expected under single hit conditions but is visible once a large amount of substrate has been used in the reaction (see the no lysate condition, [Figure 4B](#)) ([Love et al., 2012](#)). These data are consistent with previous observations that enzyme cycling, rather than processivity, is advantageous when deamination occurs in the presence of other ssDNA binding proteins, such as RPA ([Adolph et al., 2017b](#); [Wong et al., 2021](#)).

Overall, these results considered with the γ H2AX foci formation suggest that the *in vitro* data cannot be used alone to gauge activity in cells since A3A, A3B, and A3H Hap I showed different activities *in vitro* ([Figure 4](#)), but similar activities in cells as measured by γ H2AX foci ([Figures 2, 3](#)). However, since γ H2AX foci mark both dsDNA breaks and replication fork slowing, it is not known, for example, if A3A causes more DNA breaks and A3H and A3B cause only replication fork stalling due to less deaminase activity ([Rogakou et al., 1998](#); [Ward and Chen, 2001](#)). This would be consistent with A3A being identified to cause a higher mutation frequency in cancer cells and cell lines ([Petljak et al., 2022](#)). To investigate the specific effects of each A3, we determined the ability to induce common cancer phenotypes in both MCF10A and MCF7 cells. Since

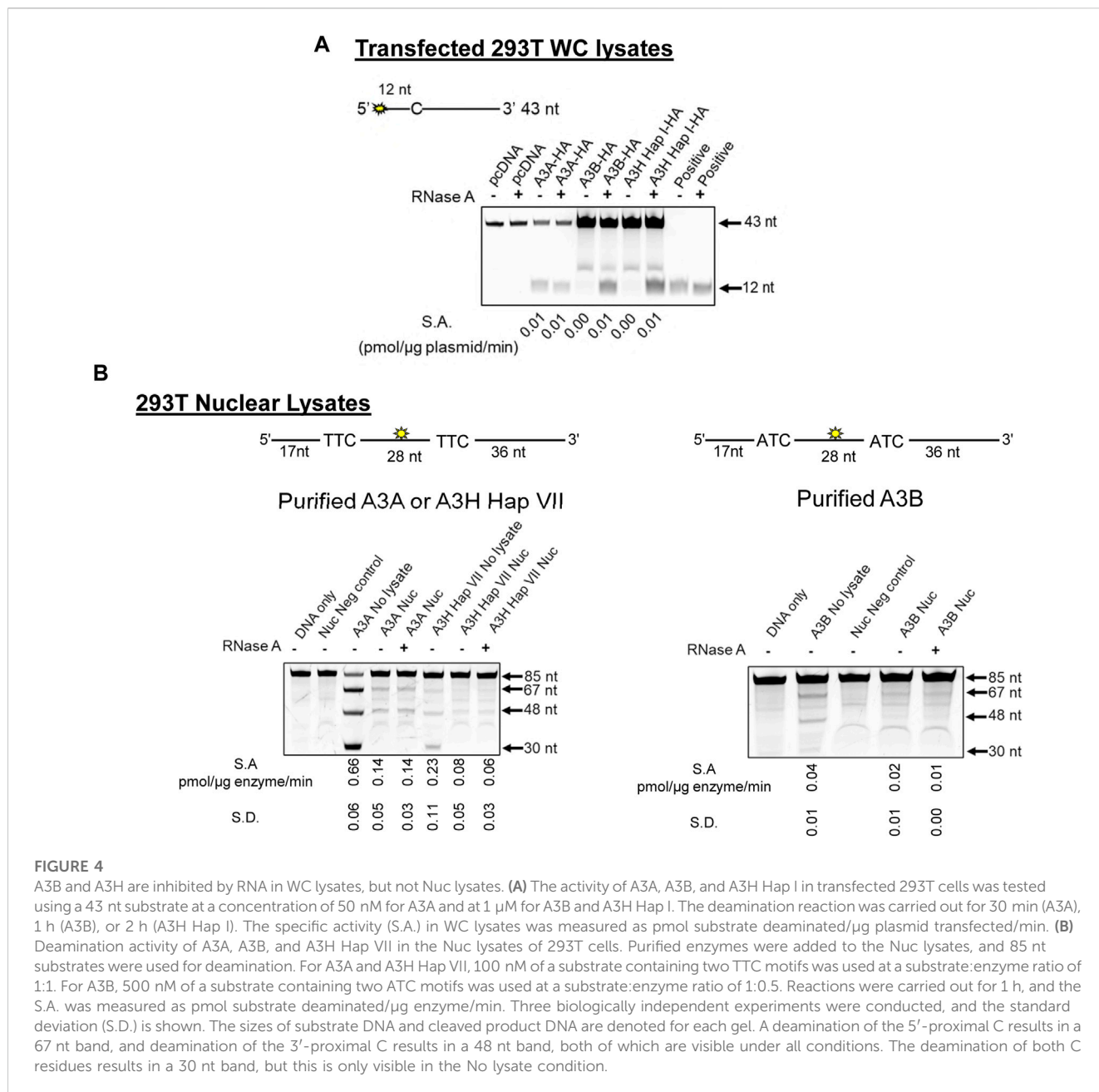


FIGURE 4

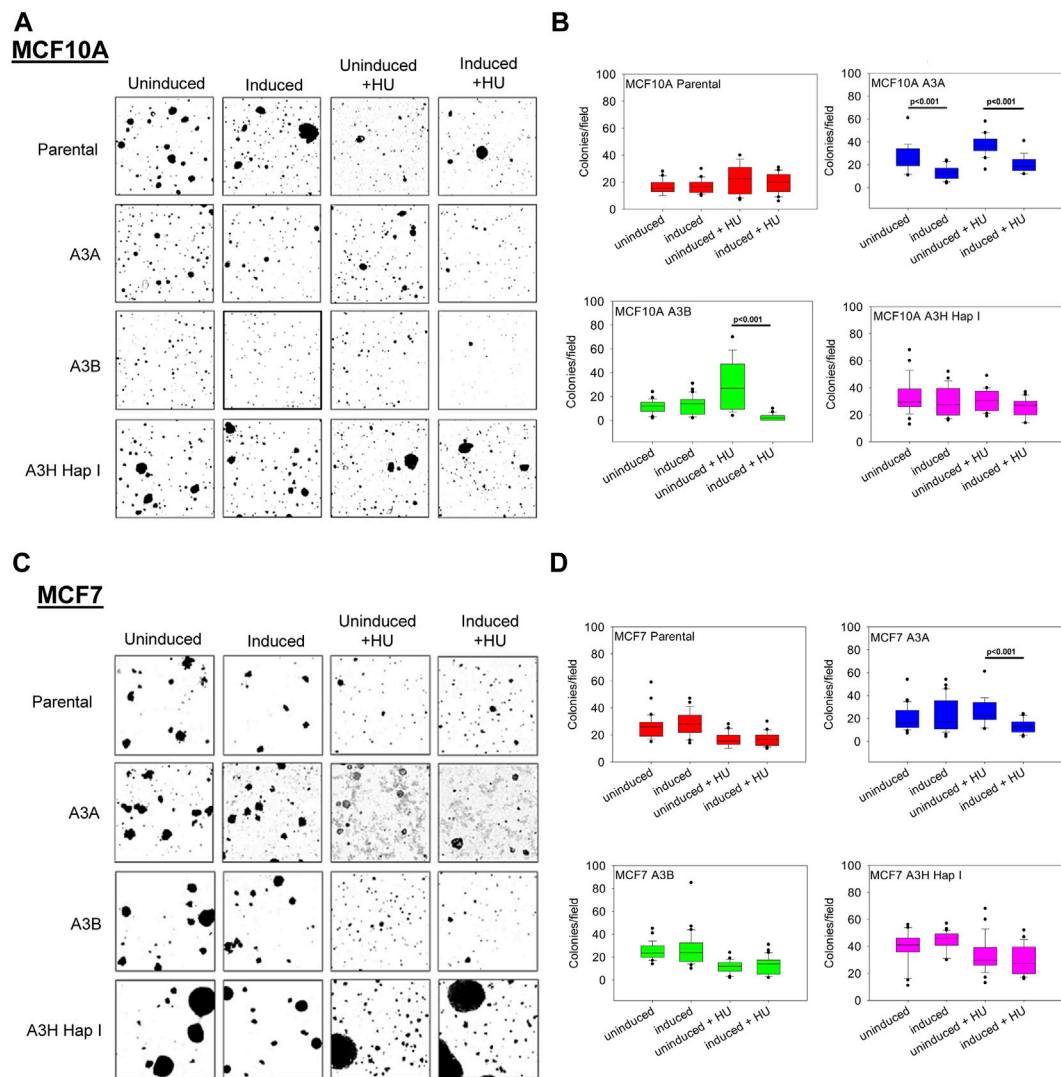
A3B and A3H are inhibited by RNA in WC lysates, but not Nuc lysates. (A) The activity of A3A, A3B, and A3H Hap I in transfected 293T cells was tested using a 43 nt substrate at a concentration of 50 nM for A3A and at 1 μM for A3B and A3H Hap I. The deamination reaction was carried out for 30 min (A3A), 1 h (A3B), or 2 h (A3H Hap I). The specific activity (S.A.) in WC lysates was measured as pmol substrate deaminated/ μg plasmid transfected/min. (B) Deamination activity of A3A, A3B, and A3H Hap VII in the Nuc lysates of 293T cells. Purified enzymes were added to the Nuc lysates, and 85 nt substrates were used for deamination. For A3A and A3H Hap VII, 100 nM of a substrate containing two TTC motifs was used at a substrate:enzyme ratio of 1:1. For A3B, 500 nM of a substrate containing two ATC motifs was used at a substrate:enzyme ratio of 1:0.5. Reactions were carried out for 1 h, and the S.A. was measured as pmol substrate deaminated/ μg enzyme/min. Three biologically independent experiments were conducted, and the standard deviation (S.D.) is shown. The sizes of substrate DNA and cleaved product DNA are denoted for each gel. A deamination of the 5'-proximal C results in a 67 nt band, and deamination of the 3'-proximal C results in a 48 nt band, both of which are visible under all conditions. The deamination of both C residues results in a 30 nt band, but this is only visible in the No lysate condition.

MCF10A is more proficient in DNA repair than MCF7 cells, especially for double-strand break repair (Francisco et al., 2008), we expected to observe cell type-specific differences.

3.4 A3A and A3B affect anchorage independent growth in soft agar

The soft agar colony formation assay is used to measure anchorage-independent growth, a hallmark of cellular transformation. We compared each cell line exposed to dox to its dox-untreated condition after 3 weeks of growth in soft agar without or with dox induction of A3 enzyme expression. In the non-tumorigenic model cell line MCF10A, no differences were

observed between the dox-treated/-untreated condition (~15 colonies) (Figures 5A,B). However, significant differences were observed for A3A-expressing cells that showed a decrease in colony formation from ~20 to ~10 colonies (Figures 5A,B). There were no significant differences observed for colonies exposed to A3B and A3H Hap I under normal replication conditions in MCF10A cells. Additionally, we tested if the effects of A3-mediated DNA damage would be amplified during replication fork stalling. Cells were either untreated or treated with dox for 24 h and subsequently treated with 2 mM HU for 6 h to induce fork stalling before plating in soft agar. Similar to the normal replication fork conditions, we did not observe differences in the number of colonies between uninduced/induced parental or A3H Hap I (Figures 5A,B). However, statistically significant differences

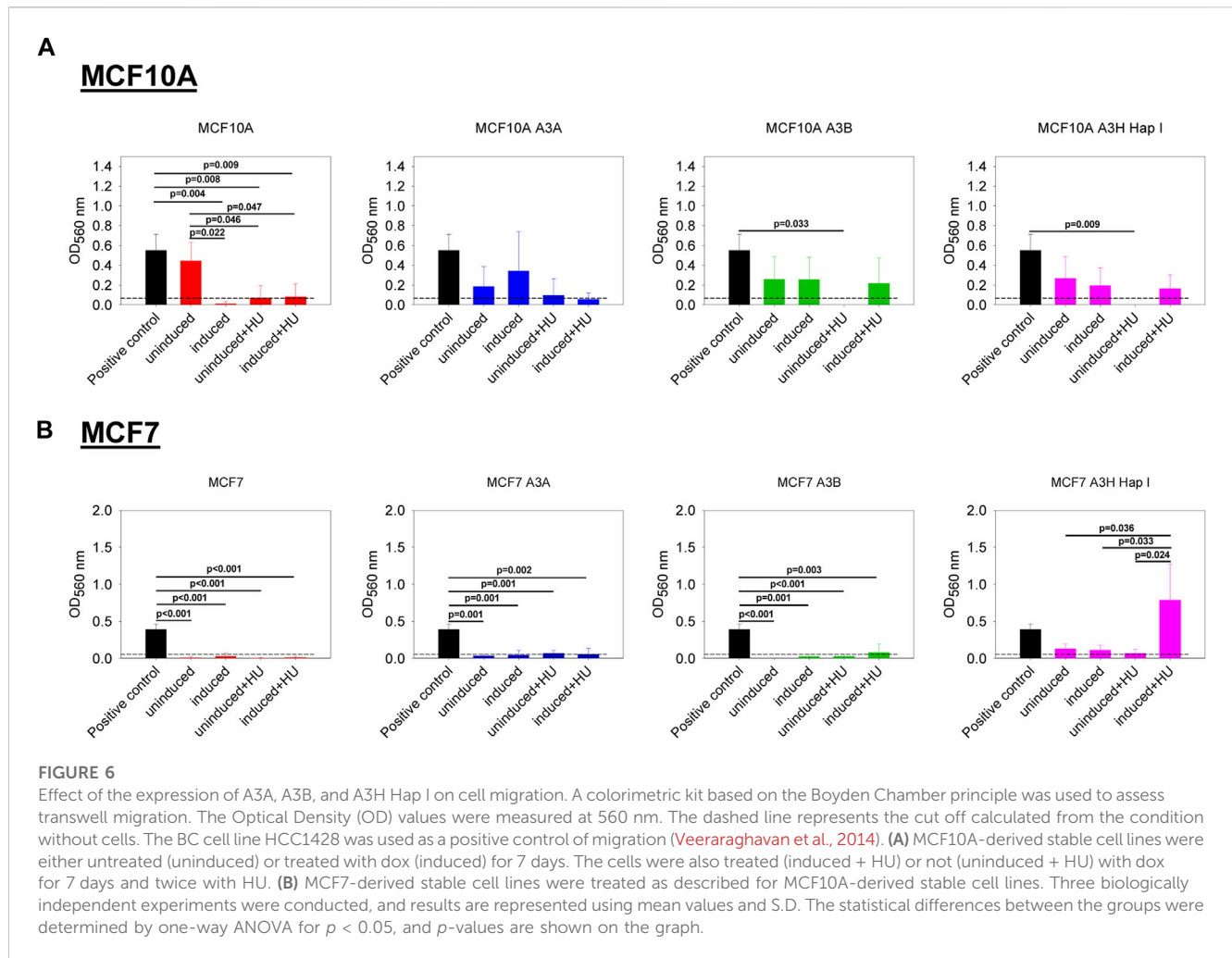
**FIGURE 5**

Effect of the expression of A3A, A3B, and A3H Hap I on anchorage-independent growth in soft agar. MCF10A and MCF7 cells were either untreated, treated with dox (0.05–2 $\mu\text{g}/\text{mL}$, 24 h), or treated with dox and HU (2 mM–12 mM, 6 h). After 3 weeks, colonies were imaged and quantified. **(A)** Representative images of colony formation in uninduced, induced, uninduced + HU, and induced + HU for MCF10A parental, A3A, A3B, and A3H Hap I cells. **(B)** Box-whisker plot of quantified uninduced, induced, uninduced + HU, and induced + HU MCF10A colonies. **(C)** Representative images of colony formation in uninduced, induced, uninduced + HU, and induced + HU for MCF7 parental, A3A, A3B, and A3H Hap I cells. **(D)** Box-whisker plot of quantified uninduced, induced, uninduced + HU, and induced + HU MCF7 colonies. Three biologically independent experiments were conducted. One representative experiment is shown in panels A and C. The statistical differences were determined by a t-test on the biologically independent experiments and considered statistically significant for $p < 0.05$.

were observed between uninduced/induced A3A and A3B. The uninduced + HU A3A condition had ~35 colonies/field in comparison to the induced + HU A3A condition, which had ~20 colonies/field. Similarly, the uninduced + HU A3B condition had ~25 colonies/field in comparison to the induced + HU A3B condition, which had <10 colonies/field. These data show that A3A and A3B have deleterious effects on soft agar colony formation in the presence of replication stress, and A3A has this effect even under normal replication conditions. This is consistent with A3A having a higher activity in Nuc lysates (Figure 4B).

We also tested the tumorigenic MCF7 breast cancer cell lines and did not observe differences in the number of colonies

between the uninduced and induced condition for parental cells or cells that expressed either A3A, A3B, or A3H Hap I (Figures 5C,D). During replication fork stalling using HU treatment, no difference in colony growth was observed between uninduced + HU and induced + HU for A3B or A3H Hap I. A3H Hap I colonies grew larger than A3B or A3A colonies, but this did not affect the total number of colonies. A statistically significant difference was observed in the A3A condition, where uninduced + HU colonies were significantly greater (~25 colonies/field) than in the induced + HU condition (~10 colonies/field). These data show that A3A expression is more deleterious to MCF7 cells when combined with replication stress (Figures 5C,D).



3.5 A3H Hap I can induce the migration of MCF7 cells

We also investigated if the expression of A3A, A3B, and A3H Hap I, either in MCF10A or MCF7 cells, could influence cell migration in the absence or presence of HU. The cell lines were not or were dox induced for 7 days, and HU was added on day 3 and day 6, as indicated in Materials and Methods. Induction of A3s with or without HU treatment had no effect on the non-tumorigenic MCF10A cells (Figure 6A). The expression of A3A and A3B, either in MCF7 breast cancer cells treated or not with HU, did not show any effect on cell migration (Figure 6B). However, for MCF7 cells, the expression of A3H Hap I in the presence of HU promoted cell migration compared to the same cells expressing A3H Hap I without HU and to the uninduced condition with or without HU (Figure 6B).

4 Discussion

The existing data implicating A3A, A3B, and A3H Hap I in cancer have led to an unclear understanding of the relative contributions of individual A3s to mutagenesis in BC (Burns

et al., 2013a; Burns et al., 2013b; Starrett et al., 2016; Cortez et al., 2019). To overcome these limitations, we developed MCF10A- and MCF7-derived stable cell lines expressing dox-inducible Flag-tagged A3A, A3B, and A3H Hap I and identified unique phenotypes for each A3. We demonstrated that all the expressed enzymes localize to the nucleus and are enzymatically active, causing UNG-dependent DNA damage. We found that *in vitro* deamination assays using WC lysates do not directly correlate with accumulation of DNA damage in cells or the extent of inhibition by cellular RNA. Altogether, the data support a model in which A3A, A3B, and A3H Hap I all induce DNA damage in normal or tumorigenic breast epithelial cells, but the phenotypic effects of the induced damage are unique for each A3.

While *in vitro* deamination in cell lysates is often used to gauge A3 activity in cells, we found inconsistencies with this method. Importantly, despite reports that A3A is a more potent inducer of DNA damage than A3B (Landry et al., 2011; Burns et al., 2013a; Mussil et al., 2013; Caval et al., 2014), our results showed that A3B and A3H Hap I could cause similar levels of γ H2AX foci as A3A (Figures 2, 3). To investigate how the deamination activity observed in cells relates to the *in vitro* deamination assay, we conducted deamination assays under various conditions. A3B and A3H Hap VII deaminated the ssDNA in the Nuc lysates as A3A does, either in

the presence or absence of RNase A (Figure 4B). This is the first direct evidence demonstrating that in the nucleus, the A3 enzymes involved in deaminating genomic DNA are still active even without the addition of RNase A.

A3B and A3H Hap VII have been previously characterized *in vitro* as processive enzymes, but we found in this study that they were non-processive on ssDNA in Nuc lysates (Figure 4B) (Feng et al., 2015; Adolph et al., 2017b). When having to compete with RPA for ssDNA, we have found that the ability of A3B and A3H Hap VII to cycle on and off DNA through intersegmental transfer, rather than the processivity (staying on the DNA and sliding or jumping), resulted in more deaminations (Adolph et al., 2017b; Wong et al., 2021; Wong et al., 2022). In addition, optimized processivity experiments in the buffer have shown that RPA can decrease the processivity of A3B and A3H Hap I by 2-fold (Adolph et al., 2017b). Studies have determined that A3 enzymes can induce clustered strand co-ordinated mutations, termed kataegis and omikli (Nik-Zainal et al., 2012; Mas-Ponte and Supek, 2020), and some suggested that for A3B, this is due to processivity (Lada et al., 2012; Maciejowski et al., 2015). However, even A3A, a non-processive enzyme, has also been found to induce kataegis and omikli in BC and other cell lines and can deaminate multiple cytosines on a single ssDNA *in vitro* when incubated for a sufficient time (Figure 4B, no lysate) (Love et al., 2012; DeWeerd et al., 2022; Petljak et al., 2022). Since kataegis and omikli are also associated with processes that create excess ssDNA, it is plausible that either processive or non-processive deaminations can result in the clustered strand co-ordinated mutations (Roberts et al., 2012; Taylor et al., 2013; Sakofsky et al., 2014; Maciejowski et al., 2020; Mas-Ponte and Supek, 2020). While our findings with A3B and A3H Hap I need to be confirmed with additional substrates in Nuc lysates, our current data indicate that their processivity is likely to be low (Figure 4B). If processivity is low under most conditions, then this is a positive feature for genome editing, where off-target deaminations at adjacent cytosines that are considered detrimental would take longer to form. It remains to be determined if in Nuc lysates RPA alone, other proteins, or other factors are limiting the processivity of A3B and A3H Hap VII.

Despite A3A being more active in Nuc lysates *in vitro*, all three enzymes had equal ability to induce γ H2AX foci in cells (Figures 2, 3). Overall, our data suggest that A3A, A3B, and A3H Hap I each contribute to cytosine deamination and DNA damage and directly show that between A3A and A3B, neither is more active in cells. However, there must be other pressures in the cells that result in a more detrimental effect of A3A on the anchorage-independent growth of cells (Figure 5) and more A3A-induced mutations being observed in cell line experiments (Petljak et al., 2022). This may be due to the ability of A3A to deaminate ssDNA in hairpin loops, which may not be protected by RPA (Brown et al., 2021; Wong et al., 2022). In contrast, A3B and A3H Hap I would need to compete for ssDNA with RPA in non-hairpin loop regions (Adolph et al., 2017b; Wong et al., 2021). Although A3 deaminase activity is stochastic, these site-specific DNA preferences and ability to compete with RPA may result in unique phenotypic markers of their promutagenic activity.

In this study, we looked for phenotypic markers of A3 expression. We observed that A3A expression could delay the anchorage-independent growth of cells in soft agar (Figure 5). A3A was most able to cause a decrease in the number of colonies formed in this assay in the presence or absence of HU in MCF10A cells or in the presence of HU in MCF7 cells (Figure 5). In contrast, A3B was only able to decrease proliferation of MCF10A cells in the presence of HU. While it might be expected that pro-carcinogenic enzymes should additionally increase the ability of the cells to grow in an anchorage-independent manner, the activity of A3 enzymes is stochastic and can result in beneficial, neutral, or detrimental cellular fates (Burns et al., 2015; Wong et al., 2022). Based on previous data which shows the tumorigenic potential of A3A, it appears that A3A may cause lethal damage to a large population of cells, but surviving ones may have tumorigenic potential (Law et al., 2020). A3A has also been found to cause deamination-independent chromosomal instability in pancreatic ductal adenocarcinoma, but only if there are existing cellular alterations, such as in the p53 function of KRAS signaling (Wörmann et al., 2021). It remains to be determined if this occurs in other cancers, such as BC. In this study, we did not find that catalytic mutants of A3A (or A3B or A3H Hap I) could cause chromosomal instability as measured by γ H2AX foci in MCF10A or MCF7 cells, although other measures of chromosomal instability remain to be tested (Figure 2).

There have been few studies that have examined A3H Hap I and its effect on cancer. The A3H mutation signature is found in lung adenocarcinomas (Starrett et al., 2016). A genetic and biochemical study showed that an A3H Hap I single-nucleotide polymorphism that destabilized the enzyme was beneficial for lung cancer, suggesting that A3H Hap I activity would be detrimental to cancer cell growth or increase immune recognition (Hix et al., 2020). However, the role of A3H in BC is less clear (Starrett et al., 2016). Our results showed that the MCF7 cells expressing A3H Hap I with pre-existing replication stress induced by HU treatment were able to migrate (Figure 6). These are the first direct evidence of the potential of A3H Hap I to contribute to a cancer cell phenotype.

In summary, we demonstrated that all three A3s are able to induce cellular phenotypes as a result of their induced DNA damage. Importantly, we showed that cytidine deamination activity for all A3s was not inhibited by RNA in Nuc lysates, and deamination-induced DNA damage was similar in cells, even with differing *in vitro* activities. These data demonstrate the importance of using accurate *in vitro* systems to determine cytidine deaminase activity and necessitate a reassessment of the contributions of A3A, A3B, and A3H Hap I to somatic mutagenesis during tumorigenesis. These data also provide more detailed deamination activity analysis for A3A, A3B, and A3H Hap I in the context of nuclear DNA that can be used in the design of base editing technologies.

Data availability statement

The original contributions presented in the study are included in the article/Supplementary Material; further inquiries can be directed to the corresponding author.

Author contributions

MGR and LC designed the study. MGR and LW performed the experiments. MGR and LC wrote the manuscript. MGR, LW, and LC edited the manuscript. All authors contributed to the article and approved the submitted version.

Funding

This work was supported by a grant to LC from the Canadian Institutes of Health Research (grant no. PJT159560) and the Postdoctoral Research Fellowship funding to MGR from the Saskatchewan Health Research Foundation.

Acknowledgments

We acknowledge Amit Gaba for critical comments during the writing of this article, Deborah Anderson for technical advice, Aimen Khan for technical support, and Arzhang Shayeganmehr for conducting the site-directed mutagenesis for the A3A and A3H Hap I catalytic mutants.

References

- Adolph, M. B., Ara, A., Feng, Y., Wittkopp, C. J., Emerman, M., Fraser, J. S., et al. (2017a). Cytidine deaminase efficiency of the lentiviral viral restriction factor APOBEC3C correlates with dimerization. *Nucleic Acids Res.* 45, 3378–3394. doi:10.1093/nar/gkx066
- Adolph, M. B., Love, R. P., Feng, Y., and Chelico, L. (2017b). Enzyme cycling contributes to efficient induction of genome mutagenesis by the cytidine deaminase APOBEC3B. *Nucleic Acids Res.* 45, 11925–11940. doi:10.1093/nar/gkx832
- Adolph, M. B., Love, R. P., and Chelico, L. (2018). Biochemical basis of APOBEC3 deoxycytidine deaminase activity on diverse DNA substrates. *ACS Infect. Dis.* 4, 224–238. doi:10.1021/acscinfed.7b00221
- Alexandrov, L. B., Nik-Zainal, S., Wedge, D. C., Aparicio, S. A., Behjati, S., Biankin, A. V., et al. (2013). Signatures of mutational processes in human cancer. *Nature* 500, 415–421. doi:10.1038/nature12477
- Alexandrov, L. B., Kim, J., Haradhvala, N. J., Huang, M. N., Tian Ng, A. W., Wu, Y., et al. (2020). The repertoire of mutational signatures in human cancer. *Nature* 578, 94–101. doi:10.1038/s41586-020-1943-3
- Arias, J. F., Koyama, T., Kinomoto, M., and Tokunaga, K. (2012). Retroelements versus APOBEC3 family members: No great escape from the magnificent seven. *Front. Microbiol.* 3, 275. doi:10.3389/fmicb.2012.00275
- Aynaud, M. M., Suspene, R., Vidalain, P. O., Mussil, B., Guetard, D., Tangy, F., et al. (2012). Human Tribbles 3 protects nuclear DNA from cytidine deamination by APOBEC3A. *J. Biol. Chem.* 287, 39182–39192. doi:10.1074/jbc.M112.372722
- Bergstrom, E. N., Luebeck, J., Petljak, M., Khandekar, A., Barnes, M., Zhang, T., et al. (2022). Mapping clustered mutations in cancer reveals APOBEC3 mutagenesis of ecDNA. *Nature* 602, 510–517. doi:10.1038/s41586-022-04398-6
- Bogerd, H. P., Wiegand, H. L., Hulme, A. E., Garcia-Perez, J. L., O'shea, K. S., Moran, J. V., et al. (2006). Cellular inhibitors of long interspersed element 1 and Alu retrotransposition. *Proc. Natl. Acad. Sci. U. S. A.* 103, 8780–8785. doi:10.1073/pnas.0603313103
- Britan-Rosich, Y., Ma, J., Kotler, E., Hassan, F., Botvinnik, A., Smith, Y., et al. (2022). APOBEC3G protects the genome of human cultured cells and mice from radiation-induced damage. *FEBS J.* 290, 1822–1839. doi:10.1111/febs.16673
- Brown, A. L., Collins, C. D., Thompson, S., Coxon, M., Mertz, T. M., and Roberts, S. A. (2021). Single-stranded DNA binding proteins influence APOBEC3A substrate preference. *Sci. Rep.* 11, 21008. doi:10.1038/s41598-021-00435-y
- Burns, M. B., Lackey, L., Carpenter, M. A., Rathore, A., Land, A. M., Leonard, B., et al. (2013a). APOBEC3B is an enzymatic source of mutation in breast cancer. *Nature* 494, 366–370. doi:10.1038/nature11881
- Burns, M. B., Temiz, N. A., and Harris, R. S. (2013b). Evidence for APOBEC3B mutagenesis in multiple human cancers. *Nat. Genet.* 45, 977–983. doi:10.1038/ng.2701
- Burns, M. B., Leonard, B., and Harris, R. S. (2015). APOBEC3B: Pathological consequences of an innate immune DNA mutator. *Biomed. J.* 38, 102–110. doi:10.4103/2319-4170.148904

Conflict of interest

The authors declare that the research was conducted in the absence of any commercial or financial relationships that could be construed as a potential conflict of interest.

Publisher's note

All claims expressed in this article are solely those of the authors and do not necessarily represent those of their affiliated organizations, or those of the publisher, the editors, and the reviewers. Any product that may be evaluated in this article, or claim that may be made by its manufacturer, is not guaranteed or endorsed by the publisher.

Supplementary material

The Supplementary Material for this article can be found online at: <https://www.frontiersin.org/articles/10.3389/fgeed.2023.1196697/full#supplementary-material>

- Caval, V., Suspene, R., Vartanian, J. P., and Wain-Hobson, S. (2014). Orthologous mammalian APOBEC3A cytidine deaminases hypermutate nuclear DNA. *Mol. Biol. Evol.* 31, 330–340. doi:10.1093/molbev/mst195
- Cescon, D. W., Haibe-Kains, B., and Mak, T. W. (2015). APOBEC3B expression in breast cancer reflects cellular proliferation, while a deletion polymorphism is associated with immune activation. *Proc. Natl. Acad. Sci. U. S. A.* 112, 2841–2846. doi:10.1073/pnas.1424869112
- Chan, K., Resnick, M. A., and Gordenin, D. A. (2013). The choice of nucleotide inserted opposite abasic sites formed within chromosomal DNA reveals the polymerase activities participating in translesion DNA synthesis. *DNA Repair (Amst)* 12, 878–889. doi:10.1016/j.dnarep.2013.07.008
- Chan, K., Roberts, S. A., Klimczak, L. J., Sterling, J. F., Saini, N., Malc, E. P., et al. (2015). An APOBEC3A hypermutation signature is distinguishable from the signature of background mutagenesis by APOBEC3B in human cancers. *Nat. Genet.* 47, 1067–1072. doi:10.1038/ng.3378
- Chen, H., Lilley, C. E., Yu, Q., Lee, D. V., Chou, J., Narvaiza, I., et al. (2006). APOBEC3A is a potent inhibitor of adeno-associated virus and retrotransposons. *Curr. Biol.* 16, 480–485. doi:10.1016/j.cub.2006.01.031
- Chen, Z., Wen, W., Bao, J., Kuhs, K. L., Cai, Q., Long, J., et al. (2019). Integrative genomic analyses of APOBEC-mutational signature, expression and germline deletion of APOBEC3 genes, and immunogenicity in multiple cancer types. *BMC Med. Genomics* 12, 131. doi:10.1186/s12920-019-0579-3
- Cheng, A. Z., Moraes, S. N., Shaban, N. M., Fanunza, E., Bierle, C. J., Southern, P. J., et al. (2021). APOBECs and herpesviruses. *Viruses* 13, 390. doi:10.3390/v13030390
- Chervova, A., Fatykhov, B., Koblov, A., Shvarov, E., Preobrazhenskaya, J., Vinogradov, D., et al. (2021). Analysis of gene expression and mutation data points on contribution of transcription to the mutagenesis by APOBEC enzymes. *Nar. Cancer* 3, zcab025. doi:10.1093/narcan/zcab025
- Chesarino, N. M., and Emerman, M. (2020). Polymorphisms in human APOBEC3H differentially regulate ubiquitination and antiviral activity. *Viruses* 12, 378. doi:10.3390/v12040378
- Cortez, L. M., Brown, A. L., Dennis, M. A., Collins, C. D., Brown, A. J., Mitchell, D., et al. (2019). APOBEC3A is a prominent cytidine deaminase in breast cancer. *PLoS Genet.* 15, e1008545. doi:10.1371/journal.pgen.1008545
- Creighton, S., Bloom, L. B., and Goodman, M. F. (1995). Gel fidelity assay measuring nucleotide misinsertion, exonucleolytic proofreading, and lesion bypass efficiencies. *Methods Enzymol.* 262, 232–256. doi:10.1016/0076-6879(95)62021-4
- De Sousa Abreu, R., Penalva, L. O., Marcotte, E. M., and Vogel, C. (2009). Global signatures of protein and mRNA expression levels. *Mol. Biosyst.* 5, 1512–1526. doi:10.1039/b908315d
- Deweerd, R. A., Nemeth, E., Poti, A., Petryk, N., Chen, C. L., Hyrien, O., et al. (2022). Prospectively defined patterns of APOBEC3A mutagenesis are prevalent in human cancers. *Cell Rep.* 38, 110555. doi:10.1016/j.celrep.2022.110555

- Evanoff, M., and Komor, A. C. (2019). Base editors: Modular tools for the introduction of point mutations in living cells. *Emerg. Top. Life Sci.* 3, 483–491. doi:10.1042/etls20190088
- Feng, Y., Baig, T. T., Love, R. P., and Chelico, L. (2014). Suppression of APOBEC3-mediated restriction of HIV-1 by vif. *Front. Microbiol.* 5, 450. doi:10.3389/fmicb.2014.00450
- Feng, Y., Love, R. P., Ara, A., Baig, T. T., Adolph, M. B., and Chelico, L. (2015). Natural polymorphisms and oligomerization of human APOBEC3H contribute to single-stranded DNA scanning ability. *J. Biol. Chem.* 290, 27188–27203. doi:10.1074/jbc.M115.666065
- Feng, Y., Goubran, M. H., Follack, T. B., and Chelico, L. (2017). Deamination-independent restriction of LINE-1 retrotransposition by APOBEC3H. *Sci. Rep.* 7, 10881. doi:10.1038/s41598-017-11344-4
- Francisco, D. C., Peddi, P., Hair, J. M., Flood, B. A., Cecil, A. M., Kalogerinis, P. T., et al. (2008). Induction and processing of complex DNA damage in human breast cancer cells MCF-7 and nonmalignant MCF-10A cells. *Free Radic. Biol. Med.* 44, 558–569. doi:10.1016/j.freeradbiomed.2007.10.045
- Friedberg, E., Walker, G., Siede, W., Wood, R., Schultz, R., and Ellenberger, T. (2005). “Base excision repair,” in *DNA repair and mutagenesis*, 169–226.
- Glaser, A. P., Fantini, D., Wang, Y., Yu, Y., Rimar, K. J., Podojil, J. R., et al. (2018). APOBEC-mediated mutagenesis in urothelial carcinoma is associated with improved survival, mutations in DNA damage response genes, and immune response. *Oncotarget* 9, 4537–4548. doi:10.18632/oncotarget.23344
- Green, A. M., and Weitzman, M. D. (2019). The spectrum of APOBEC3 activity: From anti-viral agents to anti-cancer opportunities. *DNA Repair (Amst)* 83, 102700. doi:10.1016/j.dnarep.2019.102700
- Green, A. M., Landry, S., Budagyan, K., Avgousti, D. C., Shalhout, S., Bhagwat, A. S., et al. (2016). APOBEC3A damages the cellular genome during DNA replication. *Cell Cycle* 15, 998–1008. doi:10.1080/15384101.2016.1152426
- Green, A. M., Deweerdt, R. A., O’leary, D. R., Hansen, A. R., Hayer, K. E., Kulej, K., et al. (2021). Interaction with the CCT chaperonin complex limits APOBEC3A cytidine deaminase cytotoxicity. *EMBO Rep.* 22, e52145. doi:10.15252/embr.202052145
- Henderson, S., and Fenton, T. (2015). APOBEC3 genes: Retroviral restriction factors to cancer drivers. *Trends Mol. Med.* 21, 274–284. doi:10.1016/j.molmed.2015.02.007
- Hix, M. A., Wong, L., Flath, B., Chelico, L., and Cisneros, G. A. (2020). Single-nucleotide polymorphism of the DNA cytosine deaminase APOBEC3H haplotype I leads to enzyme destabilization and correlates with lung cancer. *Nar. Cancer* 2, zcaa023. doi:10.1093/narcan/zcaa023
- Jalili, P., Bowen, D., Langenbacher, A., Park, S., Aguirre, K., Corcoran, R. B., et al. (2020). Quantification of ongoing APOBEC3A activity in tumor cells by monitoring RNA editing at hotspots. *Nat. Commun.* 11, 2971. doi:10.1038/s41467-020-16802-8
- Jarmuz, A., Chester, A., Bayliss, J., Gisbourne, J., Dunham, I., Scott, J., et al. (2002). An anthropoid-specific locus of orphan C to U RNA-editing enzymes on chromosome 22. *Genomics* 79, 285–296. doi:10.1006/geno.2002.6718
- Kanu, N., Cerone, M. A., Goh, G., Zalmas, L. P., Bartkova, J., Dietzen, M., et al. (2016). DNA replication stress mediates APOBEC3 family mutagenesis in breast cancer. *Genome Biol.* 17, 185. doi:10.1186/s13059-016-1042-9
- Kidd, J. M., Newman, T. L., Tuzun, E., Kaul, R., and Eichler, E. E. (2007). Population stratification of a common APOBEC gene deletion polymorphism. *PLoS Genet.* 3, e63. doi:10.1371/journal.pgen.0030063
- King, J. J., and Larjani, M. (2017). A novel regulator of activation-induced cytidine deaminase/APOBECs in immunity and cancer: Schrodinger’s CATalytic pocket. *Front. Immunol.* 8, 351. doi:10.3389/fimmu.2017.00351
- Komor, A. C., Kim, Y. B., Packer, M. S., Zuris, J. A., and Liu, D. R. (2016). Programmable editing of a target base in genomic DNA without double-stranded DNA cleavage. *Nature* 533, 420–424. doi:10.1038/nature17946
- Koning, F. A., Newman, E. N., Kim, E. Y., Kunstman, K. J., Wolinsky, S. M., and Malim, M. H. (2009). Defining APOBEC3 expression patterns in human tissues and hematopoietic cell subsets. *J. Virol.* 83, 9474–9485. doi:10.1128/JVI.01089-09
- Lackey, L., Demorest, Z. L., Land, A. M., Hultquist, J. F., Brown, W. L., and Harris, R. S. (2012). APOBEC3B and AID have similar nuclear import mechanisms. *J. Mol. Biol.* 419, 301–314. doi:10.1016/j.jmb.2012.03.011
- Lackey, L., Law, E. K., Brown, W. L., and Harris, R. S. (2013). Subcellular localization of the APOBEC3 proteins during mitosis and implications for genomic DNA deamination. *Cell Cycle* 12, 762–772. doi:10.4161/cc.23713
- Lada, A. G., Dhar, A., Boissy, R. J., Hirano, M., Rubel, A. A., Rogozin, I. B., et al. (2012). AID/APOBEC cytosine deaminase induces genome-wide kataegis. *Biol. Direct* 7, 47. doi:10.1186/1745-6150-7-47
- Landry, S., Narvaiza, I., Linfesty, D. C., and Weitzman, M. D. (2011). APOBEC3A can activate the DNA damage response and cause cell-cycle arrest. *EMBO Rep.* 12, 444–450. doi:10.1038/embor.2011.46
- Law, E. K., Sieuwerts, A. M., Lapara, K., Leonard, B., Starrett, G. J., Molan, A. M., et al. (2016). The DNA cytosine deaminase APOBEC3B promotes tamoxifen resistance in ER-positive breast cancer. *Sci. Adv.* 2, e1601737. doi:10.1126/sciadv.1601737
- Law, E. K., Levin-Klein, R., Jarvis, M. C., Kim, H., Argyris, P. P., Carpenter, M. A., et al. (2020). APOBEC3A catalyzes mutation and drives carcinogenesis *in vivo*. *J. Exp. Med.* 217, e20200261. doi:10.1084/jem.20200261
- Li, M. M., and Emerman, M. (2011). Polymorphism in human APOBEC3H affects a phenotype dominant for subcellular localization and antiviral activity. *J. Virol.* 85, 8197–8207. doi:10.1128/JVI.00624-11
- Liu, Z., Chen, S., Shan, H., Jia, Y., Chen, M., Song, Y., et al. (2020). Precise base editing with CC context-specificity using engineered human APOBEC3G-nCas9 fusions. *BMC Biol.* 18, 111. doi:10.1186/s12915-020-00849-6
- Liu, W., Newhall, K. P., Khani, F., Barlow, L., Nguyen, D., Gu, L., et al. (2023). The cytidine deaminase APOBEC3G contributes to cancer mutagenesis and clonal evolution in bladder cancer. *Cancer Res.* 83, 506–520. doi:10.1158/0008-5472.CAN-22-2912
- Love, R. P., Xu, H., and Chelico, L. (2012). Biochemical analysis of hypermutation by the deoxycytidine deaminase APOBEC3A. *J. Biol. Chem.* 287, 30812–30822. doi:10.1074/jbc.M112.393181
- Maciejowski, J., Li, Y., Bosco, N., Campbell, P. J., and De Lange, T. (2015). Chromothripsis and kataegis induced by telomere crisis. *Cell* 163, 1641–1654. doi:10.1016/j.cell.2015.11.054
- Maciejowski, J., Chatziplis, A., Dananberg, A., Chu, K., Toufekhtan, E., Klimczak, L. J., et al. (2020). APOBEC3-dependent kataegis and TREX1-driven chromothripsis during telomere crisis. *Nat. Genet.* 52, 884–890. doi:10.1038/s41588-020-0667-5
- Mas-Ponte, D., and Supek, F. (2020). DNA mismatch repair promotes APOBEC3-mediated diffuse hypermutation in human cancers. *Nat. Genet.* 52, 958–968. doi:10.1038/s41588-020-0674-6
- Mcgrath, E., Shin, H., Zhang, L., Phue, J. N., Wu, W. W., Shen, R. F., et al. (2019). Targeting specificity of APOBEC-based cytosine base editor in human iPSCs determined by whole genome sequencing. *Nat. Commun.* 10, 5353. doi:10.1038/s41467-019-13342-8
- Mertz, T. M., Harcy, V., and Roberts, S. A. (2017). Risks at the DNA replication fork: Effects upon carcinogenesis and tumor heterogeneity. *Genes (Basel)* 8, 46. doi:10.3390/genes8010046
- Middlebrooks, C. D., Banday, A. R., Matsuda, K., Udquim, K. I., Onabajo, O. O., Paquin, A., et al. (2016). Association of germline variants in the APOBEC3 region with cancer risk and enrichment with APOBEC-signature mutations in tumors. *Nat. Genet.* 48, 1330–1338. doi:10.1038/ng.3670
- Milewska, A., Kindler, E., Vokovski, P., Zeglen, S., Ochman, M., Thiel, V., et al. (2018). APOBEC3-mediated restriction of RNA virus replication. *Sci. Rep.* 8, 5960. doi:10.1038/s41598-018-24448-2
- Mussil, B., Suspene, R., Aynaud, M. M., Gauvrit, A., Vartanian, J. P., and Wain-Hobson, S. (2013). Human APOBEC3A isoforms translocate to the nucleus and induce DNA double strand breaks leading to cell stress and death. *PLoS One* 8, e73641. doi:10.1371/journal.pone.0073641
- Nik-Zainal, S., Alexandrov, L. B., Wedge, D. C., Van Loo, P., Greenman, C. D., Raine, K., et al. (2012). Mutational processes molding the genomes of 21 breast cancers. *Cell* 149, 979–993. doi:10.1016/j.cell.2012.04.024
- Nik-Zainal, S., Wedge, D. C., Alexandrov, L. B., Petljak, M., Butler, A. P., Bolli, N., et al. (2014). Association of a germline copy number polymorphism of APOBEC3A and APOBEC3B with burden of putative APOBEC-dependent mutations in breast cancer. *Nat. Genet.* 46, 487–491. doi:10.1038/ng.2955
- Nowarski, R., Wilner, O. I., Cheshin, O., Shahar, O. D., Kenig, E., Baraz, L., et al. (2012). APOBEC3G enhances lymphoma cell radioresistance by promoting cytidine deaminase-dependent DNA repair. *Blood* 120, 366–375. doi:10.1182/blood-2012-01-402123
- Oh, S., Bournique, E., Bowen, D., Jalili, P., Sanchez, A., Ward, I., et al. (2021). Genotoxic stress and viral infection induce transient expression of APOBEC3A and pro-inflammatory genes through two distinct pathways. *Nat. Commun.* 12, 4917. doi:10.1038/s41467-021-25203-4
- Okeoma, C. M., Huegel, A. L., Lingappa, J., Feldman, M. D., and Ross, S. R. (2010). APOBEC3 proteins expressed in mammary epithelial cells are packaged into retroviruses and can restrict transmission of milk-borne virions. *Cell Host Microbe* 8, 534–543. doi:10.1016/j.chom.2010.11.003
- Petljak, M., and Alexandrov, L. B. (2016). Understanding mutagenesis through delineation of mutational signatures in human cancer. *Carcinogenesis* 37, 531–540. doi:10.1093/carcin/bgw055
- Petljak, M., Alexandrov, L. B., Brummel, J. S., Price, S., Wedge, D. C., Grossmann, S., et al. (2019). Characterizing mutational signatures in human cancer cell lines reveals episodic APOBEC mutagenesis. *Cell* 176, 1282–1294. doi:10.1016/j.cell.2019.02.012
- Petljak, M., Dananberg, A., Chu, K., Bergstrom, E. N., Striepen, J., Von Morgen, P., et al. (2022). Mechanisms of APOBEC3 mutagenesis in human cancer cells. *Nature* 607, 799–807. doi:10.1038/s41586-022-04972-y
- Refsland, E. W., and Harris, R. S. (2013). The APOBEC3 family of retroelement restriction factors. *Curr. Top. Microbiol. Immunol.* 371, 1–27. doi:10.1007/978-3-642-37765-5_1
- Refsland, E. W., Stenglein, M. D., Shindo, K., Albin, J. S., Brown, W. L., and Harris, R. S. (2010). Quantitative profiling of the full APOBEC3 mRNA repertoire in lymphocytes

- and tissues: Implications for HIV-1 restriction. *Nucleic Acids Res.* 38, 4274–4284. doi:10.1093/nar/gkq174
- Richardson, S. R., Narvaiza, I., Planegger, R. A., Weitzman, M. D., and Moran, J. V. (2014). APOBEC3A deaminates transiently exposed single-strand DNA during LINE-1 retrotransposition. *Elife* 3, e02008. doi:10.7554/eLife.02008
- Roberts, S. A., and Gordenin, D. A. (2014). Hypermutation in human cancer genomes: Footprints and mechanisms. *Nat. Rev. Cancer* 14, 786–800. doi:10.1038/nrc3816
- Roberts, S. A., Sterling, J., Thompson, C., Harris, S., Mav, D., Shah, R., et al. (2012). Clustered mutations in yeast and in human cancers can arise from damaged long single-strand DNA regions. *Mol. Cell* 46, 424–435. doi:10.1016/j.molcel.2012.03.030
- Roelofs, P. A., Timmermans, M. a. M., Stefanovska, B., Den Boestert, M. A., Van Den Borne, A. W. M., Balcioglu, H. E., et al. (2023). Aberrant APOBEC3B expression in breast cancer is linked to proliferation and cell cycle phase. *Cells* 12, 1185. doi:10.3390/cells12081185
- Rogakou, E. P., Pilch, D. R., Orr, A. H., Ivanova, V. S., and Bonner, W. M. (1998). DNA double-stranded breaks induce histone H2AX phosphorylation on serine 139. *J. Biol. Chem.* 273, 5858–5868. doi:10.1074/jbc.273.10.5858
- Roper, N., Gao, S., Maity, T. K., Banday, A. R., Zhang, X., Venugopalan, A., et al. (2019). APOBEC mutagenesis and copy-number alterations are drivers of proteogenomic tumor evolution and heterogeneity in metastatic thoracic tumors. *Cell Rep.* 26, 2651–2666. doi:10.1016/j.celrep.2019.02.028
- Sakofsky, C. J., Roberts, S. A., Malc, E., Mieczkowski, P. A., Resnick, M. A., Gordenin, D. A., et al. (2014). Break-induced replication is a source of mutation clusters underlying kataegis. *Cell Rep.* 7, 1640–1648. doi:10.1016/j.celrep.2014.04.053
- Serebrenik, A. A., Starrett, G. J., Leenen, S., Jarvis, M. C., Shaban, N. M., Salamango, D. J., et al. (2019). The deaminase APOBEC3B triggers the death of cells lacking uracil DNA glycosylase. *Proc. Natl. Acad. Sci. U. S. A.* 116, 22158–22163. doi:10.1073/pnas.1904024116
- Shi, K., Carpenter, M. A., Banerjee, S., Shaban, N. M., Kurahashi, K., Salamango, D. J., et al. (2017). Structural basis for targeted DNA cytosine deamination and mutagenesis by APOBEC3A and APOBEC3B. *Nat. Struct. Mol. Biol.* 24, 131–139. doi:10.1038/nsmb.3344
- Sieuwerths, A. M., Willis, S., Burns, M. B., Look, M. P., Meijer-Van Gelder, M. E., Schlicker, A., et al. (2014). Elevated APOBEC3B correlates with poor outcomes for estrogen-receptor-positive breast cancers. *Horm. Cancer* 5, 405–413. doi:10.1007/s12672-014-0196-8
- St Martin, A., Salamango, D., Serebrenik, A., Shaban, N., Brown, W. L., Donati, F., et al. (2018). A fluorescent reporter for quantification and enrichment of DNA editing by APOBEC-Cas9 or cleavage by Cas9 in living cells. *Nucleic Acids Res.* 46, e84. doi:10.1093/nar/gky332
- Starrett, G. J., Luengas, E. M., Mccann, J. L., Ebrahimi, D., Temiz, N. A., Love, R. P., et al. (2016). The DNA cytosine deaminase APOBEC3H haplotype I likely contributes to breast and lung cancer mutagenesis. *Nat. Commun.* 7, 12918. doi:10.1038/ncomms12918
- Swanton, C., Mcgranahan, N., Starrett, G. J., and Harris, R. S. (2015). APOBEC enzymes: Mutagenic fuel for cancer evolution and heterogeneity. *Cancer Discov.* 5, 704–712. doi:10.1158/2159-8290.CD-15-0344
- Talluri, S., Samur, M. K., Buon, L., Kumar, S., Potluri, L. B., Shi, J., et al. (2021). Dysregulated APOBEC3G causes DNA damage and promotes genomic instability in multiple myeloma. *Blood Cancer J.* 11, 166. doi:10.1038/s41408-021-00554-9
- Taylor, B. J., Nik-Zainal, S., Wu, Y. L., Stebbings, L. A., Raine, K., Campbell, P. J., et al. (2013). DNA deaminases induce break-associated mutation showers with implication of APOBEC3B and 3A in breast cancer kataegis. *Elife* 2, e00534. doi:10.7554/eLife.00534
- Veeraraghavan, J., Tan, Y., Cao, X. X., Kim, J. A., Wang, X., Chammess, G. C., et al. (2014). Recurrent ESR1-CCDC170 rearrangements in an aggressive subset of oestrogen receptor-positive breast cancers. *Nat. Commun.* 5, 4577. doi:10.1038/ncomms5577
- Veira, V. C., and Soares, M. A. (2013). The role of cytidine deaminases on innate immune responses against human viral infections. *Biomed. Res. Int.* 2013, 683095. doi:10.1155/2013/683095
- Vogel, C., and Marcotte, E. M. (2012). Insights into the regulation of protein abundance from proteomic and transcriptomic analyses. *Nat. Rev. Genet.* 13, 227–232. doi:10.1038/nrg3185
- Wang, W., and Malcol, B. A. (1999). Two-stage PCR protocol allowing introduction of multiple mutations, deletions and insertions using QuikChange Site-Directed Mutagenesis. *Biotechniques* 26, 680–682. doi:10.2144/99264st03
- Wang, X., Abudu, A., Son, S., Dang, Y., Venta, P. J., and Zheng, Y. H. (2011). Analysis of human APOBEC3H haplotypes and anti-human immunodeficiency virus type 1 activity. *J. Virol.* 85, 3142–3152. doi:10.1128/JVI.02049-10
- Ward, I. M., and Chen, J. (2001). Histone H2AX is phosphorylated in an ATR-dependent manner in response to replicational stress. *J. Biol. Chem.* 276, 47759–47762. doi:10.1074/jbc.C100569200
- Wei, Y., Silke, J. R., Aris, P., and Xia, X. (2020). Coronavirus genomes carry the signatures of their habitats. *PLoS One* 15, e0244025. doi:10.1371/journal.pone.0244025
- Wong, L., Vizeacoumar, F. S., Vizeacoumar, F. J., and Chelico, L. (2021). APOBEC1 cytosine deaminase activity on single-stranded DNA is suppressed by replication protein A. *Nucleic Acids Res.* 49, 322–339. doi:10.1093/nar/gkaa1201
- Wong, L., Sami, A., and Chelico, L. (2022). Competition for DNA binding between the genome protector replication protein A and the genome modifying APOBEC3 single-stranded DNA deaminases. *Nucleic Acids Res.* 50, 12039–12057. doi:10.1093/nar/gkac1121
- Wörmann, S. M., Zhang, A., Thege, F. I., Cowan, R. W., Rupani, D. N., Wang, R., et al. (2021). APOBEC3A drives deaminase domain-independent chromosomal instability to promote pancreatic cancer metastasis. *Nat. Cancer* 2, 1338–1356. doi:10.1038/s43018-021-00268-8
- Yan, S., He, F., Gao, B., Wu, H., Li, M., Huang, L., et al. (2016). Increased APOBEC3B predicts worse outcomes in lung cancer: A comprehensive retrospective study. *J. Cancer* 7, 618–625. doi:10.7150/jca.14030
- Zhao, D., Li, J., Li, S., Xin, X., Hu, M., Price, M. A., et al. (2021). Glycosylase base editors enable C-to-A and C-to-G base changes. *Nat. Biotechnol.* 39, 35–40. doi:10.1038/s41587-020-0592-2